Received: 11 February 2023 | Revised: 22 May 2023 | Accepted: 26 May 2023

DOI: 10.1002/pc.27483

RESEARCH ARTICLE

Polymer COMPOSITES WILEY

Waterborne polymer composites containing hybrid graphene/carbon nanotube filler: Effect of graphene type on properties and performance

Marija Prosheva[1,2] | **Maryam Ehsani**[1,3] | **Yvonne Joseph**[3] | **Radmila Tomovska**[1,4] | **Jadranka Blazhevska Gilev**[2]

[1]POLYMAT and Departamento de Química Aplicada Facultad de Ciencias Químicas University of the Basque Country, Joxe Mari Korta Center, Donostia-San Sebastian, Spain

[2]Faculty of Technology and Metallurgy, Ss. Cyril and Methodius University in Skopje, Skopje, Macedonia

[3]Technische Universität Bergakademie Freiberg, Institute of Electronic and Sensor Materials, Freiberg, Germany

[4]Ikerbasque Basque Foundation for Science, Bilbao, Spain

Correspondence
Jadranka Blazhevska Gilev, Faculty of Technology and Metallurgy, Ss. Cyril and Methodius University in Skopje, Ruger Boskovic 16 1000 Skopje, Macedonia.
Email: jadranka@tmf.ukim.edu.mk

Abstract

Polymer composites based on graphene/carbon nanotubes (G/CNT) and reduced graphene oxide/carbon nanotubes (rGO/CNT) were synthetized by in-situ miniemulsion polymerization containing 1 wt% hybrid filler with different ratio of G and CNT (10:1, 1.1, 1:10). From the hybrid aqueous dispersions obtained in that way polymer films were spontaneously formed at ambient conditions by water evaporation. The effect of the type of the graphene filler, G or rGO, on the properties and performance of polymer composites was studied. It was shown that G/CNT based composites presented improved morphology of the film due to better distribution of the filler and more organized structure of the film than that of rGO/CNT composites. The surface of the film was much smoother indicating more deepen filler within the polymer. Consequently, the G/CNT/polymer composites presented one order of magnitude increased Young's moduli and 60% lower water uptake than the neat polymer. Even though rGO/CNT/polymer composites presented also improved mechanical resistance, their water resistance was compromised probably due to the presence of hydrophilic functional groups that facilitated the water diffusion within the film.

KEYWORDS

miniemulsion, G/CNT hybrids, rGO/CNT hybrids, waterborne composites

1 | INTRODUCTION

Graphene (G) and carbon nanotubes (CNT) are very well-known advanced materials, widely investigated for different applications, including for synthesis of nanocomposites. When these materials are used as fillers in polymer composites, they affect importantly the final properties of the composite.[1] Both, G and CNTs are built from sp^2 hybridized carbon atoms, with important difference in their architecture. G is 2D platelet like structure, whereas CNTs are 1D tube-like structure. These features are responsible for the different interactions of G and CNTs with the polymer matrix and the performance of the composite. Nevertheless, for both of them the main challenge for the development of full potential of the polymer composites is their tendency to agglomerate by van der Waals interactions and strong incompatibility with majority of the polymer matrices.[2–4] When G platelets and CNT aggregate importantly, they are impeded to create a continuous network within the polymer matrix which decreases the capacity to efficiently convey their excellent properties to the composites.

Marija Prosheva and Maryam Ehsani contributed equally.

One strategy to overcome these challenges might be to mix G and CNTs prior to their addition to the polymer to form three-dimensional network within the polymer matrix.[5,6] In these hybrid structures, the G and CNTs are connected by π–π interactions, and have shown to improve electrical, mechanical and thermal properties, in addition to the mutual stabilizing effects. These effects diminish the tendency of the carbon nanomaterial to form aggregates, and improve the dispersion of the filler within the polymer matrix.[5–10] Such composites made of hybrid G/CNT filler have shown to provide to the composite novel characteristics and to widen their application potential. For example, the improved charge transfer process within the G/CNT hybrids improved the photostability of (meth)acrylic waterborne composites up to 400 h at accelerated aging conditions.[6] Xiang et al. reported strain sensor based on G/CNT/poly(urethane) composites with higher sensitivity, larger detectable range, and cycle stability.[10] The enhanced performance was attributed to the synergistic effect of CNTs and G that improved dispersion of CNTs in polymer matrix, as well as the electrical and tensile properties of the sensor. The enhanced electrical conductivity of the composites containing G/CNT hybrids compared to the composites containing individual filler either G or CNTs was employed by Zhang et al. to unlocked application of composites as electromagnetic interference shielding coatings.[11] The excellent properties that these hybrid structures possess make them suitable filler for synthesis of polymer composites with different properties and wide application, for example, protective coatings,[6,11] sensors[10] etc.

We published comprehensive review of the graphene-based polymer composites, in which the state-of-the art was analyzed comprehensively until 2017.[2] In recent years, a lot of work has been done on developing water borne coatings containing different types of graphene fillers, given that solvent borne coatings not only pollute the environment but also pose a serious threat to human health.[12,13] Carbon nanomaterials, as a result of their excellent mechanical and chemical properties, represent a suitable filler for obtaining composite coatings with superior properties.[14–17] By incorporation of graphene filler within waterborne epoxy resin, the anticorrosion properties were improved.[16,18,19] The synthesis of the composite coatings was done by mixing solution containing graphene filer with epoxy resin. Prior the composite synthesis the graphene was modified. For instance, Zhu et al were able to improve the anticorrosion properties of waterborne epoxy resin by incorporation of graphene oxide/polyaniline filler.[16] Lignin-OH/graphene dispersion was mixed with epoxy resin by Wang et al,[18] they obtained good anticorrosion properties by adding 0.5 wt% of the filler within the epoxy resin. Remarkable anticorrosion and barrier properties were reported by Zhou et al.[19] They attributed the improved properties of the epoxy-based composite to the well Lysine-modified graphene oxide.[19] Wang et al obtained poly(urethane-acrylate) anticorrosion coatings reinforced with reduced graphene oxide functionalized with titanate by in-situ polymerization.[20] The results suggested that composites possess excellent long-term corrosion resistance.[20] Similarly, Zhang et al, synthetized coating based on waterborne polyurethane and graphene, where the polyurethane pre-polymer was mixed with triethylene tetramine-polyethylene glycol diglycidyl ether functionalized graphene oxide.[21] The reported results suggest that not only the composites presented good anticorrosion properties, but also, good adhesion to a substrate.[21] Polyacrylic acid modified graphene oxide was used as filler in the synthesis of waterborne polyurethane coating. The composite coating was synthetised by mixing a graphene solution with waterborne polyurethane. The obtained coating, not only that presented improved mechanical properties, but also it had notable abrasion durability, as the mass loss rate was decreased by 77.1%.[17]

To the authors best knowledge, there are not reports on the synthesis of waterborne polymer composites with G/CNT filler with potential application as water protective coating. Usually the synthesis of G/CNT/polymer nanocomposites is based on solution blending or mixing.[7,11,22–24] Conventionally organic solvents as dimethylformamide (DMF)[7,22,23] or tetrahydrofurane (THF)[11] are used, which means that during the film formation the organic solvents evaporate increasing the content of volatile organic vapors in the environment. This is one of the largest drawbacks of these synthesis methods. Besides, often thermal treatment at temperatures from 70 to 200°C[10,11,22–24] are implemented either to dissolve the polymer[24] or to induce precipitation,[11] drying,[10,11,22,23] annealing,[24] or mixing of the nanomaterial and the polymer.[22] Carbon nanomaterial hybrid/resin composites were prepared in similar manner, by dispersion of the pristine carbon nanomaterial[25] within the resin, in ethanol,[26] THF[27] or water[28] followed by degasification[25] or removal of the solvent by drying in oven,[26–28] and finally by curing the resin at temperatures between 60 and 160°C.[25–27]

There are reports on solvent-free synthesis of the polymer composites based on hybrid carbon, such as melt extrusion,[29] melt compounding,[30] hot compaction (compression)[31,32] or fused filament fabrication 3D printing,[10] however, these techniques are usually time and energy consuming and the aggregation of the filler is more pronounced.

Between other disadvantages is that the solution mixing or melt blending and extrusions methods do not

provide always a uniform dispersion of the filler within the polymer matrix, which negatively influence the properties of the composite.[2,33]

According to relatively recent review,[2] the polymerization methods performed in heterogeneous media, preferably water, appears as suitable alternative for synthesis of composite materials. Except much more environmentally friendly solvent (water), these techniques offer much better control of the composites characteristics and especially they provide platform of enhanced dispersions of the nanomaterial filler in the matrix. Namely, after synthesis a hybrid aqueous dispersions are produced, in which the nanomaterial is distributed in the interstitial spaces between the polymer nanoparticles, which prevent the nanomaterial aggregation during composite film preparation from such aqueous dispersions.[34,35] Similar process has been implemented by Patole et al. to functionalize G/CNT hybrids by styrene, in microemulsion polymerization process. Such functionalized hybrids were afterwards used to synthesize styrene-based composites by solution mixing process. According to this, the use of solvents was not avoided, and moreover the whole technique was multistep, time and energy consuming.[35] Considering that aqueous polymers are mostly used for adhesives, coatings and paints applications, it is of great importance that the method of synthesis be fast and with lower costs.[34]

Encouraged by our previous successful synthesis of (meth)acrylic polymer composites based on G/CNT hybrids for UV protective coating by miniemulsion polymerization in situ process,[6] in the present work we implemented similar synthesis procedure with main aim of creation of polymer composites for high performance application. Moreover, two types of graphene material were combined with multiwall CNTs (MWCNT) prior to their introduction in the polymer composites. On one hand, graphene powder with average thickness of the platelets of 8 nm was used and on the other, reduced graphene oxide produced by chemical reduction GO (single layer thick) in aqueous dispersions. The main difference between G and rGO is the surface functionalization. As a consequence of the partial reduction achieved chemically, rGO remains more functionalized compared to the G. G or rGO were then mixed in different weight ratios with CNT in aqueous dispersions. The dispersions were used as water phase to prepare a miniemulsion with selected (meth)acrylic monomers, which was polymerized afterwards. For that aim methyl methacrylate (MMA) and butyl acrylate (BA) monomer mixture in 1:1 weight ratio was selected to ensure glass transition temperature (T_g) of the resulting polymer lower than ambient temperature. Consequently, the resulting hybrid aqueous dispersion made of polymer nanoparticles and G/CNTs or rGO/CNTs would be film-forming. This means that, after casting the dispersion on a substrate, a continuous composite film will be spontaneously formed by water evaporation. As previously demonstrated in case of graphene fillers, this way of composites creation offers decreased aggregation and improved dispersion of the nanomaterial in the polymer matrix due to the fact that nanomaterial is placed in the interstitial space between the individual polymer nanoparticles, which allows decreasing the content of nanomaterials without compromising the performance.[2] Consequently, such composites are built with very low carbon nanomaterial content (few percentage), offering very large interfacial area between the phases,[36–38] making the technique even more economic. In situ polymerization in dispersed media offers much more intimate contact between the phases during the polymerization process, resulting in formation of covalent bonds between the two phases and impressive reinforcing effect.[34,37,39]

Film forming hybrid aqueous dispersions were obtained, from which composite films were prepared spontaneously by water evaporation at ambient conditions. Their mechanical and water uptake performance was investigated.

2 | EXPERIMENTAL SECTION

2.1 | Materials

Multiwalled carbon nanotubes (CNT, length = 5–15 μm and diameter = 10–30 nm) were purchased from Sigma Aldrich. Single layer graphene oxide dispersed in water (GO, 5 mg/mL, thickness <1 nm, average lateral platelets size of 500 nm) was acquired from ACS Material, and graphene nanopowder (G, 8 nm thick flakes, with lateral dimension of 5 μm and purity of 99.9% from Graphene Supermarket, USA). Sodium dodecyl sulfate (SDS) was used as surface-active reagent for dispersion of the powder in double distillated water was purchased from Sigma Aldrich (purity 98%). Polyvinylpyrrolidone (PVP) from Sigma Aldrich was used for dispersion of CNT in the GO dispersion. Ascorbic acid from Acros organics was used for reduction of GO into reduced graphene oxide (rGO).

For the synthesis of the nanocomposites the following monomers were used: methyl methacrylate (MMA) (purity 99.9%) from Qumidroga, buthyl acrylate (BA) (purity 99.5%) from Qumidroga, glycidyl methacrylate (GMA) (purity 97%) from Acros organic. Initiator potassium persulfate (KPS) from Sigma Aldrich (purity 99%), initiator azobisisobutyronitrile (AIBN) from Sigma Aldrich (purity 98%), surfactant Dowfax 2A1 solution 45% (alkyldiphenyloxide disulfonate) from Dow chemical

company and co-stabilizer stearyl acrylate (SA) from BASF (purity 98%) were used for synthesis of the different composites and the neat polymer. During all experiments Milli-Q® ultrapure water was used. A redox couple initiator was used for post-polymerization process, ascorbic acid from Acros organics and tert-Butyl hydroperoxide (70% solution in H2O) from Sigma Aldrich were used for preparation of the redox couple initiator.

2.2 | Methods

2.2.1 | Preparation of G/CNTs hybrid nanomaterial

The G/CNT hybrids in three different weight ratios (G:CNT of 10:1; 1:1; and 1:10) were prepared following procedures explained elsewhere.[5,6] Shortly, graphene and CNT in suitable amounts (Table S1) were sonicated (Branson 450 instrument, Danbury, CT) in air according the following parameters: 70% of power output and 50% duty cycle for 90 min efficient time, under continuous stirring with magnetic stirrer of 200 rpm.

The obtained G/CNT hybrids were dispersed in water using SDS as a surface active agent. The SDS (0.25 g) and water (50 g) were stirred for 30 min, and then 0.25 g of G/CNT powder of all ratios was added in the mixture and was sonicated 10 min under continuous stirring. The sonication parameters were the same as mentioned previously.

2.2.2 | Preparation of rGO/CNTs hybrid

The rGO/CNT hybrids in three different weight ratios (rGO:CNT of 10:1, 1:1 and 1:10) were prepared in aqueous dispersion by sonication (Branson 450 instrument, Danbury, CT). The procedure started by sonication of appropriate amount of GO aqueous dispersion (Table S2). The sonication was performed under the following conditions: 80% power output and 50% duty cycle for 15 min efficient time, under continuous agitation with magnetic stirrer of 200 rpm. The CNTs in appropriate amounts (Table S2) were sonicated separately in air medium under the following conditions: 70% power output and 50% duty cycle for 90 min efficient time, under mixing with magnetic stirrer of 200 rpm.

Afterwards, the two dispersions were mixed and sonicated with 70% power output and 50% duty cycle for 2.5 min efficient time, under mixing with magnetic stirrer of 200 rpm.

In order to obtain reduced graphene oxide, the GO/CNT hybrids were subjected to reduction. The reduction was performed as it follows: first PVP 5 wt% was added to the GO/CNT hybrid aqueous dispersions and was left stirring for 30 min. Then ascorbic acid was added with the ratio of solids to reductant of 5:1. Afterwards, the rGO/CNT mixtures were placed in an oven at 90°C and kept for 60 min. After the reduction, all three samples were subjected do dialysis to remove the excess of PVP. The dialysis was performed using molecular weight cut-off membrane (MWCO): Spectrum labs with 12–14,000 Daltons, the process was carried out for 1 week, the pH was measured regularly and the water was changing, until was obtained a stable pH.

2.2.3 | In situ miniemulsion polymerization

Two series of composites were synthetized by in-situ miniemulsion, one of them based on 1 wt% of the G/CNT hybrids, and the other based on 1 wt% of the rGO/CNT hybrids.

20% solids content (s.c.) miniemulsion was prepared by mixing aqueous phase containing dispersed G/CNT or rGO/CNT hybrids in presence of surfactant Dowfax 2A1 (2 wt% based on monomers (b.m.)) and the oil phase consisting of monomer mixture MMA, BA, GMA (49.5/49.5/1 weight ratio) and co-stabilizer stearyl acrylate (SA 6 wt% b.m.), added to prevent miniemulsion droplet diffusional degradation (Oswald ripening). The MMA/BA ratio (1:1 by weight) is selected to keep the glass transition temperature of the final polymer bellow room temperature, which allow continuous composite film formation at atmospheric conditions by water evaporation. GMA in 1 wt% with respect to MMA/BA is used as a functional monomer to make the polymer chains more compatible with the carbon nanomaterial.

In Tables 1 and 2, the formulations for synthesis of G/CNT and rGO/CNT hybrid dispersions with 20% solid content (s.c), respectively are presented.

The emulsion formed by mixing of both phases was sonicated (Branson 550 instrument, Danbury, CT) at 70% power output, 50% duty cycle under magnetic stirring for 15 min efficient time and in iced water bath. The resulting thermodynamically stable miniemulsion was polymerized in batch mode for 60 min at 70°C, under N_2 bubbling, using KPS (0.5 wt% b.m.). When rGO was used, full monomer conversion was achieved in all cases. The systems polymerized in presence of G presented low monomer conversion, especially when 10:1 and 1:1 G/CNT were employed. As already observed and reported previously,[6] these hybrids are efficient scavenger of free radicals, which decreased the efficiency of the free-radical polymerization process. Hence, these two reactions were subjected to post-polymerization using redox couple initiator prepared using ascorbic acid and tert-butyl hydroperoxide, each of them in concentration of 0.5 wt% b.m. The process was performed

TABLE 1 Formulation for preparation of 20% s.c. hybrid latexes containing G/CNT hybrids.

Water phase (grams)				Oil phase (grams)			
G/CNT Aqueous dispersion 1 wt%[a]	Distillated water	Dowfax 2 wt%[a]	Initiator 0.5 wt%[a]	MMA	BA	GMA	SA 6 wt%[a]
50	24.2	0.37	0.093	9.16	9.16	0.185	1.11

[a]Based on monomers.

TABLE 2 Formulation for synthesis of 20% s.c. hybrid latexes containing rGO/CNT hybrids.

	Water phase (grams)				Oil phase (grams)			
Sample	rGO/CNT Aqueous dispersion 1 wt%[a]	Double Distillated water	Dowfax 2 wt%[a]	Initiator 0.5 wt%[a]	MMA	BA	GMA	SA 6 wt%[a]
1 wt% 10:1	10.4	70	0.4	0.1	9.9	9.9	0.2	1.2
1 wt% 1:1	7.4	73	0.4	0.1	9.9	9.9	0.2	1.2
1 wt% 1:10	5.0	75.4	0.4	0.1	9.9	9.9	0.2	1.2

[a]Based on monomers.

under mild agitation, at 20°C, for 48 h. Full monomer conversion was achieved in case of 1:10 G/CNTs. Nevertheless, the reaction with 10:1 hybrid again was not successful. Hence, polymerization was performed using oil soluble initiator. AIBN is oil soluble initiator that creates free radicals in oil phase. Therefore, the direct contact between the hybrid filler placed in aqueous phase and the free radicals was avoided, finally resulting in creation of composite dispersions with full monomer conversion.

After the polymerization, the dispersions containing 1 wt% 1:10 G/CNT and 1 wt% 1:10 rGO/CNT presented high percentage of coagulum, 17% and 25%, respectively. The films were formed at standard atmospheric conditions (25°C and 55% relative humidity) from all the dispersions, including the one with coagulum, which was removed prior to film preparation. At Figure 1, it can be noticed that the films obtained from the dispersions containing 1 wt% of G/CNT and rGO/CNT with ratio of 1:10 are almost transparent. This indicates that large filler fractions were placed within the coagulum. Therefore, these composites were not investigated further.

The neat copolymer was also synthetized by miniemulsion polymerization, according the formulation presented in the Tables 1 and 2, where instead of aqueous dispersion of G/CNT or rGO/CNT, surfactant aqueous solution was used.

2.3 | Characterization

Transmission electron microscopy (TEM) equipped with LaB6 filament (TECNAI G2 20 TWIN) was employed to observe the structure of the mixed nanocarbon materials G/CNT with different ratios between both. The hybrid and the neat dispersions were cut by die cutter for further analysis. FTIR equipped with ATR (Perkin Elmer Spectrum 100) was used to study the pristine G, CNT, GO and the rGO/CNT hybrids before and after reduction. For analysis of the FTIR spectra OMNIC software was used.

In order to observe the morphology of the cross-section of the composite films, the films were frozen in liquid nitrogen and broken. The cross-section of the films was investigated by scanning electron microscopy (SEM) (Quanta 250 e-SEM, Philips Tecna).

TopoMetrix Discoverer (TMX-2010) cantilever Atomic force microscopy (AFM) with silicon nitride (Si3N4) was employed to study the surface of the composite films. The samples for AFM analysis were prepared by cutting the composite films in appropriate specimens (10 mm × 10 mm × 0.5 mm). Gwyddion software was used for analysis of the AFM images.

To investigate the mechanical properties of the composites, the films with approximate thickness of 0.5 mm were cut in appropriate tensile test specimens (15 mm × 3.5 mm × 0.5 mm). The mechanical properties were determined by tensile test, following ASTM D3039. The Tensile test was carried out with TA.HD plus texture analyzer (Stable Micro Systems Ltd., Godalming, UK) with a constant strain velocity of 1.5 mm s^{-1}. The length between the jaws was 15 mm and the nominal strain rate in the experiments was 0.1 Hz. Using Microsoft Excel functions, the Young's modulus and Offset Yield were estimated.

The surface chemical composition of each composite was examined with X-ray photoelectron spectroscopy (XPS). The probes were prepared by drop casting on

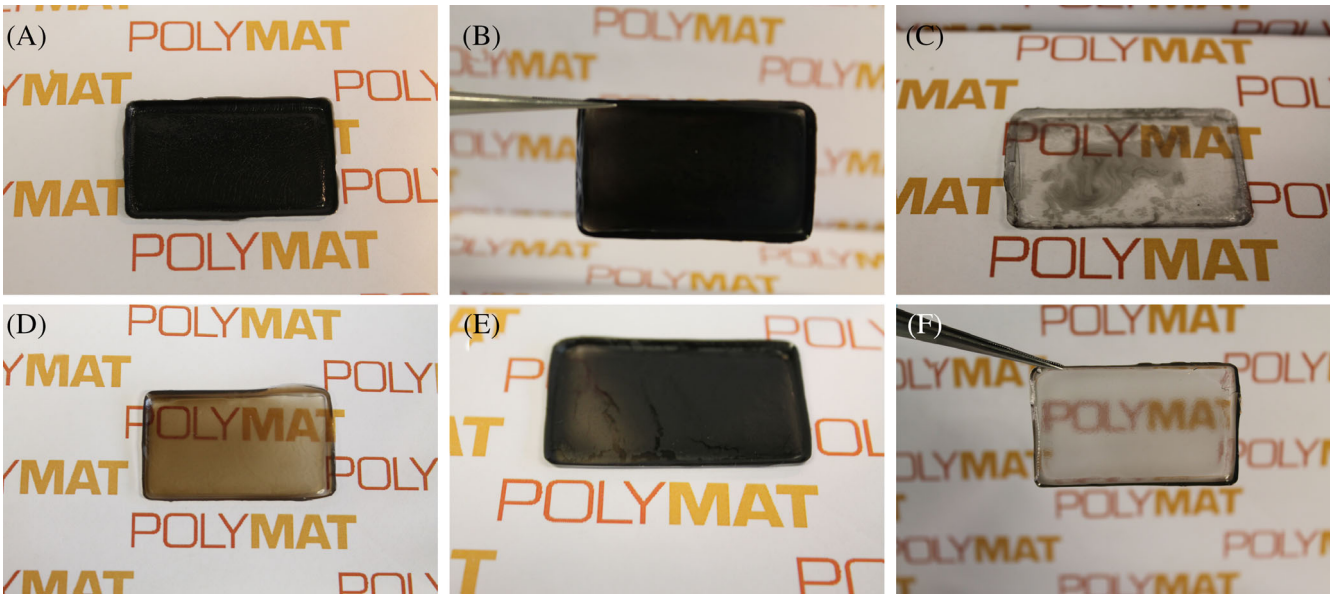

FIGURE 1 Photos of the composite films containing 1% of: (A) 10:1 G/CNT/polymer, (B) 1:1 G/CNT/polymer, (C) 1:10 G/CNT/polymer, (D) 10:1 rGO/CNT/polymer, (E) 1:1 rGO/CNT/polymer, and (F) 1:10 rGO/CNT/polymer.

silicon substrates. The XPS analysis was carried out with Thermo Fisher ESCALAB 250Xi XPS spectrometer, Al Kalpha (1486.6 eV) as X-ray source. The pass energy was set to 100 eV for the survey spectra and 10 eV for the detailed XPS spectra.

The water uptake of the neat polymer and the composites was investigated by immersion of the samples into distillated water at room temperature. The water uptake experiments were conducted following ASTM D570-98. Before immersion the mass of the samples was weight, in order to study the reproducibility of the aging process, the testing was triplicated. The progress was monitored by measuring the mass of the samples at certain time intervals during 300 h. The samples were removed from the water at various time intervals, the water drops on the surfaces of the samples were cleared off and then the samples were weighed. The percentage of mass change was calculated with Equation (1).

$$\text{Mass change}\,(\%) = \frac{M_t - M_0}{M_0} \times 100 \qquad (1)$$

3 | RESULTS AND DISCUSSIONS

Before the preparation of the hybrids, FTIR spectra of the pristine G, GO and CNT were recorded, the spectra are given in Figure S1. On the spectra of the G and CNT, was observed peak that correspond to the C═C vibrational stretching (1600–1500 cm^{-1}), whereas, on the GO spectrum the characteristic bands of the hydroxyl group (3700–3000 cm^{-1}), carbonyl group (1710 cm^{-1}) and from the C═C (1600 cm^{-1}) can be observed.

In order to investigate the effect of the graphene type within the G/CNT hybrid filler, two types of hybrids were prepared. The first one was prepared by sonication of graphene and CNT mixtures in different weight ratios between the both, performed in air. To enable easier incorporation of these hybrids within the polymer matrix, the hybrid was dispersed in water using SDS surfactant. The second hybrid type was prepared by sonication of mixtures of GO and CNT in different ratios in aqueous dispersion. The GO is amphiphilic material made of hydrophobic carbon-based platelets decorated with oxygen functional groups that provide hydrophilicity, especially on the edges. This structure allowed π–π bonds establishing between the aromatic structures of CNT and GO, while the oxygen functional groups provide good dispersibility of this hybrid nanomaterial in water. Afterwards, the reduction of the GO was performed in presence of PVP as steric stabilizer in order to maintain the stable aqueous dispersion after significant removal of the oxygen functionalities during the reduction process. Previous experience has shown that PVP is excellent stabilizer for rGO in aqueous dispersion and compatibilizer with the MMA/BA phase.[2,34,36–38,40] It is worth mentioning that it was intended to stabilize colloidally the G/CNT dispersions using PVP, but without success, probably due to the much higher hydrophobicity of G relatively to rGO. The structure of the prepared hybrids, investigated by TEM, is shown in Figure 2. It can be seen that the graphene (Figure 2A–C) is further exfoliated

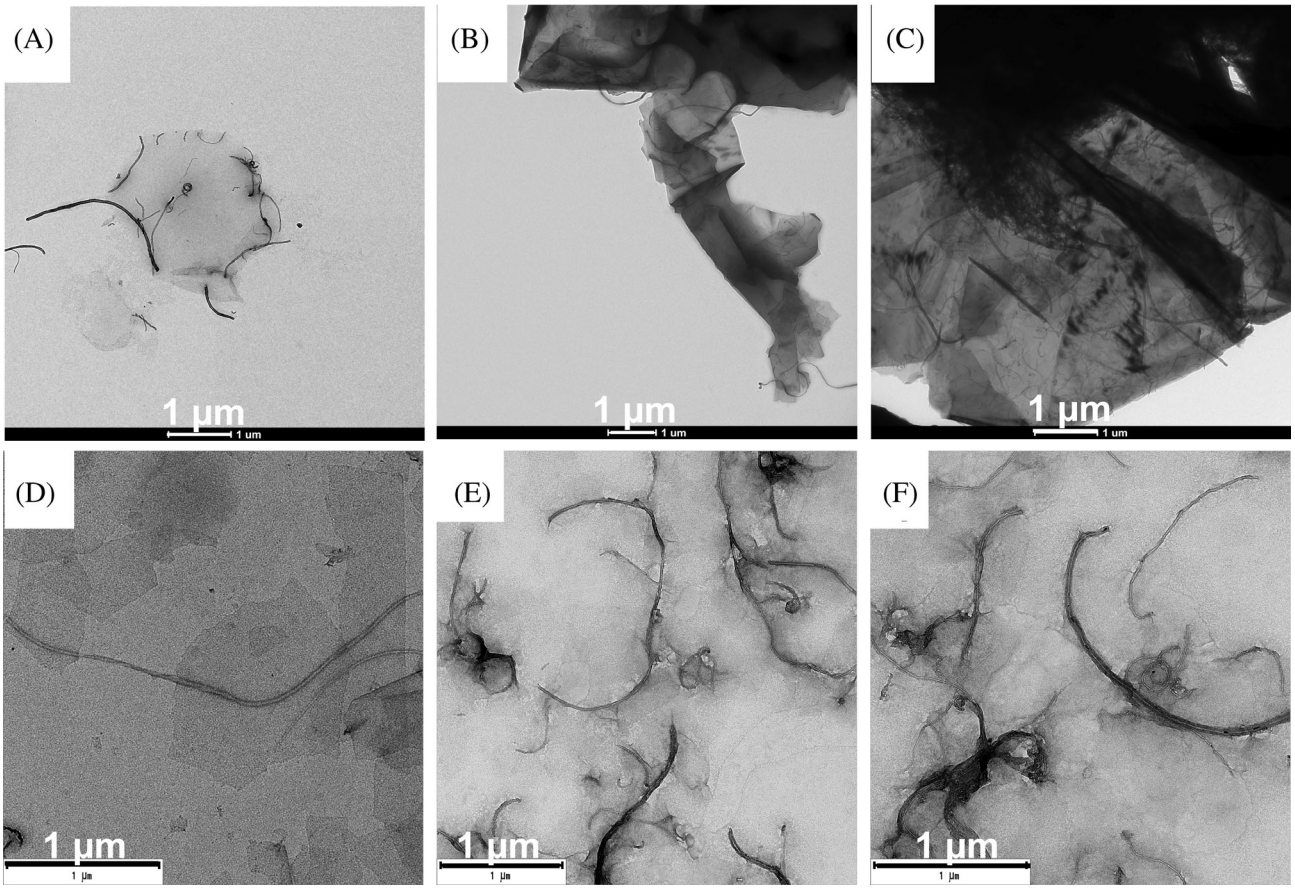

FIGURE 2 TEM images of (A) 10:1 G/CNT, (B) 1:1 G/CNT, (C) 1:10 G/CNT, (D) 10:1 rGO/CNT, (E) 1:1 rGO/CNT and (F) 1:10 rGO/CNT hybrids.

during the preparation of the hybrids by sonication, as transparent platelets can be observed, especially at lower CNT fraction (10:1) for both G and rGO. With the increment of the CNTs fraction in the hybrids, the G and rGO platelets restacked more, as they lost the transparency in the TEM images, but as well the presence of small CNT bundles might be noticed. The aggregation is more pronounced in the hybrids containing G, which is not surprising, taking into account its high hydrophobicity. From the images, it can be noticed as well that the CNTs are not only distributed on the surface of the G and rGO platelets, but they act as connecting wires between multiple platelets. The hybrids based on rGO are less aggregated, probably due to the slight hydrophilic character provided by the residual oxygen groups. In Figure S2, the FTIR spectra of the rGO/CNT hybrids before and after reduction are given. On the spectra were observed the characteristic bands of GO that originate from the hydroxyl group (3700–3100 cm^{-1}), carbonyl group (1700 cm^{-1}) and from the C═C (1620 cm^{-1}). After reduction, the intensities of the hydroxyl and carbonyl peaks decreased suggesting reduction of the GO. As GO was chemically reduced, the residual oxygen within rGO was in the range of 13%–18%,[41,42] according to similar research work. The rGO present smaller lateral dimensions, which is likely due to the characteristics of the starting materials. The 10:1 hybrids present larger graphene aggregation, whereas 1:10 large nanotubes bundles. It seems that in 1:1 hybrids, both fillers are well exfoliated, which increases largely the interface between the both.

In order to obtain composite film with satisfactory properties that will enable appropriate application of the composite, the hybrid should be well dispersed through the polymer matrix. Both hybrid types G/MCNTs and rGO/CNTs were introduced within the aqueous phase of emulsion prepared by dispersing MMA/BA/GMA monomer mixture in water, which was miniemulsified by sonication and polymerized afterwards. Hybrid aqueous dispersions containing polymer nanoparticles and hybrid fillers were produced. As already mentioned, the hybrid dispersions containing 1:10 ratio fillers contained large quantity of coagulum, therefore they were not investigated. The hybrid dispersions that contain 1:1 and 10:1 hybrid filler ratio were casted in silicon molds and dried at standard atmospheric

conditions ($T = 25°C$ and 55% relative humidity). After water evaporation nice composite films were obtained as shown in Figure 1. The morphology of the composites was investigated using SEM and the results are presented in Figure 3, where the cross-section of the films of G/CNT/polymer and rGO/CNT/polymer composites is shown. The structures with bright color are representing the G(rGO)/CNT hybrids and the dark surface refers to the polymer matrix.

The distribution of the filler within the polymer matrix is affected by the type of the graphene used and, by the hybrid ratio between both graphene and nanotubes. For 10:1 ratio G and rGO to nanotubes, from the TEM images in Figure 2, it was observed that the 10:1 hybrids had the best exfoliation of the platelets, which positively affected the morphology of the composites. In the SEM image of 10:1 G/CNT composite (Figure 3A) dark areas represent the polymer matrix, and the brighter gray areas represent the hybrid filler. The diameter of the polymeric area is around 100–250 nm, which correspond to the size of a polymer particle, which are surrounded by the filler structures. In this sample, presence of large aggregates of the hybrid was not noticed. In the cross-section of the composite reinforced with 10:1 rGO/CNT, the hybrid (Figure 3c) is homogenously dispersed throughout the polymer matrix. Mostly platelet like structures are observed with average diameter of 500 nm, corresponding to the size of original GO, which are oriented perpendicularly to the top surface of the film. The morphology of the composites is clearly affected by the type of graphene material. Even though rGO is more hydrophilic and provides improved compatibility with polymer, G probably established stronger p–p interactions with CNT. Probably such more homogeneous filler is responsible for improved distribution of G/CNT within the polymer matrix. Similar observation was found in Figure 3B,D where 1:1 ratio fillers are investigated. In case of G/CNT hybrid the distribution is improved.

The surface morphology of the nanocomposites has important influence of their properties and future application. Therefore, the surface was characterized by AFM and by XPS to determine both, the morphology and the roughness, but as well the chemistry. The AFM images of the G/CNT/polymer and rGO/CNT/polymer composites are presented in Figure 4, whereas, Table 3 presents the root mean square roughness. The top surface of all the films creates different roughness that depends on the type of graphene and the ratio of the hybrid. Figure 4 shows that G/CNT hybrids provide smoother surface to the composite that rGO/CNT, indicating that the G hybrids are more deepen in the polymer matrix than rGO hybrids. On the other hand, 1:1 ratio hybrids created

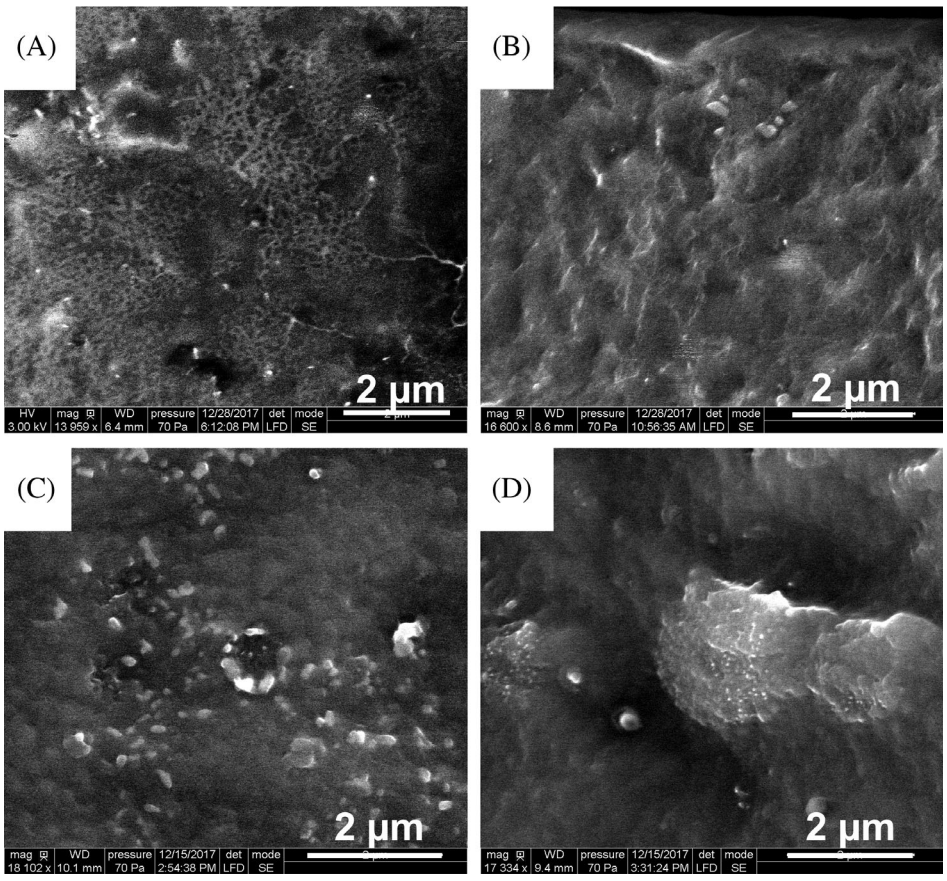

FIGURE 3 SEM images of the (A) 10:1 G/CNT/polymer, (B) 1:1 G/CNT/polymer, (C) 10:1rGO/CNT/polymer, (D) 1:1 rGO/CNT/polymer.

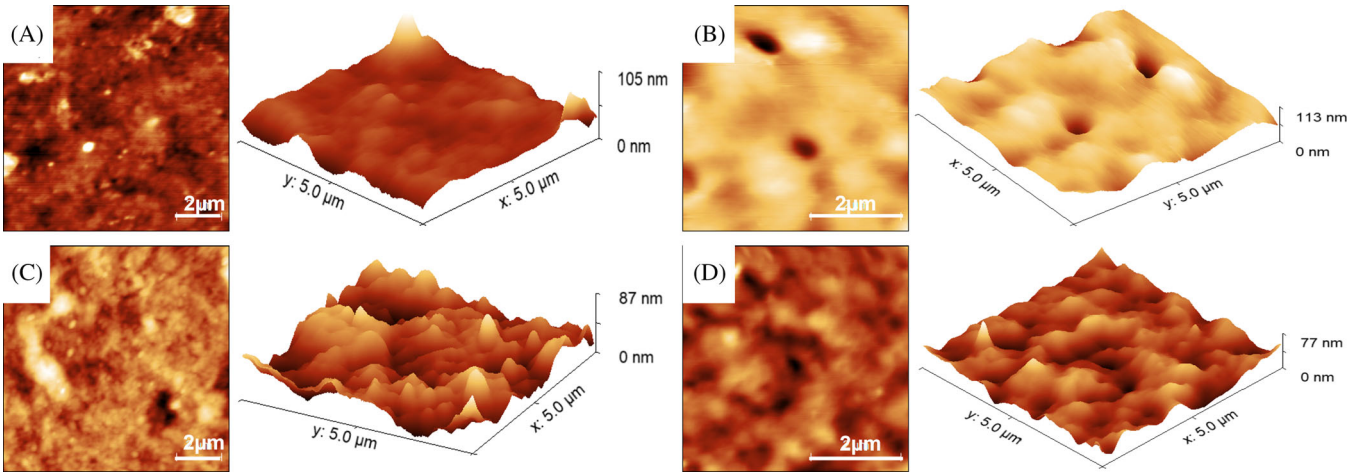

FIGURE 4 AFM height images and 3D version of the height images of composites: (A) 10:1 G/CNT/polymer, (B) 1:1 G/CNT/polymer, (C) 10:1 rGO/CNT/polymer, (D) 1:1 rGO/CNT/polymer).

rougher surface than 10:1, which means that, higher quantity of 1:1 fillers (both G and rGO) is placed on the composite-air surface providing the composite samples with larger surface area and richer phase interface. This result is related to the hydrophobicity of the hybrid fillers. Namely, during film formation by water evaporation, the more hydrophilic structures will move toward the film–air interface. Whereby, the less hydrophilic will stay deeper in the polymer matrix, creating films different in roughness and morphology. Moreover, the surface roughness and composition will determine the properties of the film in applications as coatings or paints, such as gloss for example, which will be higher for smoother film and the interaction of the composite films with impurities.

The chemical composition of the composite surface was investigated by XPS. The neat polymer and the composites presented similar surface composition. The presence of the following elements was detected: potassium (K), sodium (Na), sulfur (S) and carbon (C), which originate from the used initiator (KPS) and surfactant (SDS) (Table S3). The XPS results are shown in Figure 5 for composite materials and in Figure S3 in Supporting Information for neat polymer.

The O (1s) spectra of the neat polymer (Figure S3) and the G/CNTs composites (Figure 5A2,B2) are quite similar to each other, with broad peak at 531 eV that corresponds to C═O and C—O, originated from the polymer. This is in accordance to roughness results that indicated that composites based on G/CNT hybrids are smoother and the filler is deepen within the polymer. On the other hand, O (1s) spectra of the rGO/CNT/polymer composite (Figure 5C2,D2) present additional peak at 533 eV that corresponds to C—O—H,[43,44] which originates from the incomplete reduction of rGO. This is additional proof

TABLE 3 Root mean square roughness (RMS) for the composites.

Sample	RMS roughness (nm)
10:1 G/CNT/polymer	9.78 ± 4.31
1:1 G/CNT/polymer	19.22 ± 4.77
10:1 rGO/CNT/polymer	23.65 ± 9.10
1:1 rGO/CNT/polymer	18.92 ± 9.59

that in the rGO/CNT composites the filler is present on the surface making it to be rougher. The curve fitting of C (1s), Figure 1S for neat polymer and Figure 5A3–D3 for the composites, reveals a high intensity peak at binding energy of 285 eV which corresponds to C—C and C—H, and a peak at 288 eV that corresponds to O—C═O.

The chemical composition in relative at% of the samples is similar for all of them is presented in Table S3, Supporting information.

In order to investigate the influence of G/CNT and rGO/CNT filler on the mechanical properties of the films, tensile measurements were performed, including the neat polymer film, synthesized under the same conditions as the composites. The stress–strain curves for the neat polymer and the different composites are presented in Figure 6. Table S4 in supporting information presents the modulus and the other mechanical characteristic.

By addition of small amount (1 wt%) of hybrid filler much stiffer composites were produced. The Young's moduli of the G/CNT polymer composites improved five-fold, whereas the same quantity of rGO/CNT hybrid resulted in one order of magnitude higher moduli. This difference is likely result on the compatibility between the hybrid filler and the polymer matrix. The presence of the residual oxygen functional groups onto rGO

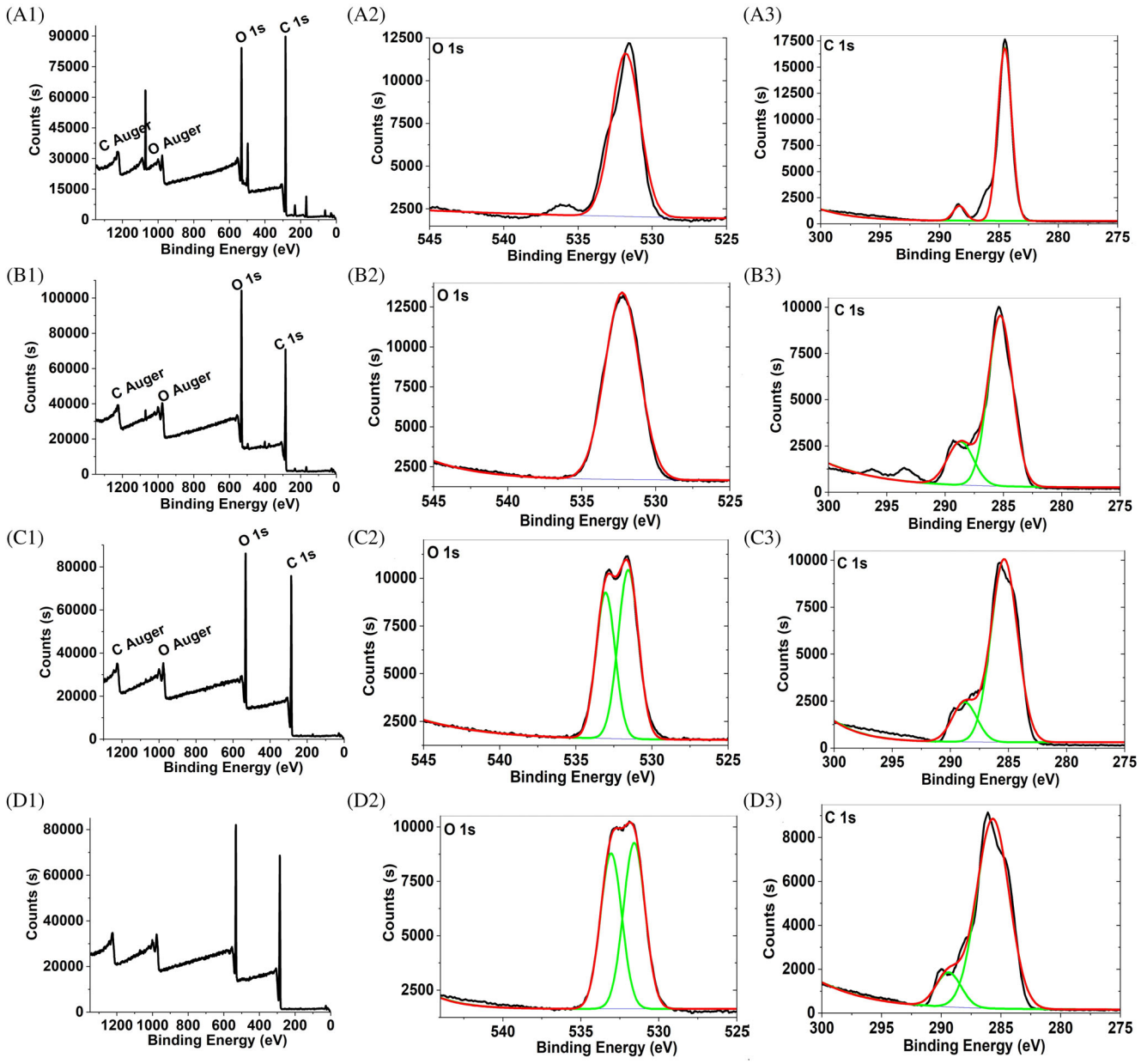

FIGURE 5 XPS survey spectra obtained on the surface of the (A1–A3) 10:1 G/CNT/polymer, (B1–B3) 1:1 G/CNT/polymer, (C1–C3) 10:1 rGO/CNT/polymer, and (D1–D3) 1:1 rGO/CNT/polymer.

interacted physically and chemically with the polymer matrix, as we demonstrated previously, introducing even covalent crosslinking.[23] On the other hand, this crosslinking decreases the mobility of the filler within the matrix. It is worth mentioning that the composites 10:1 G/CNT/polymer present very high elongation at break. Even though the composites are less flexible than the neat polymer as shown in Figure 6, the flexibility lost is negligible for this composite, taking into consideration the higher moduli. The much higher value of the Young's moduli of the composites compared to the neat polymer suggests that the hybrid efficiently limits the movement of the polymer chains making the samples less flexible as well the stress is efficiently transferred from the polymer matrix to the filler. The offset yield stress of the composites is 4.5 times higher than the neat polymer for the G/CNT samples and 6 times higher for the rGO/CNT samples. This means that the composites will undergo permanent deformation at higher stress. Overall, the higher Young's modulus and offset yield stress suggest that the material will be long-lasting and more resistant to applied mechanical stress.

The reinforcing effect of the carbon nanomaterial incorporated within polymer matrix is due to the high aspect ratio of the carbon nanomaterials that enables efficient transfer of stress from the polymer matrix to the

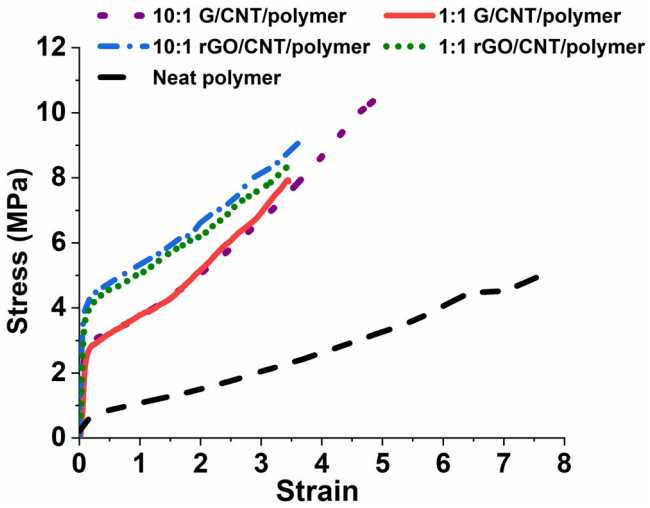

FIGURE 6 Stress–strain behavior of the neat polymer and different composite films.

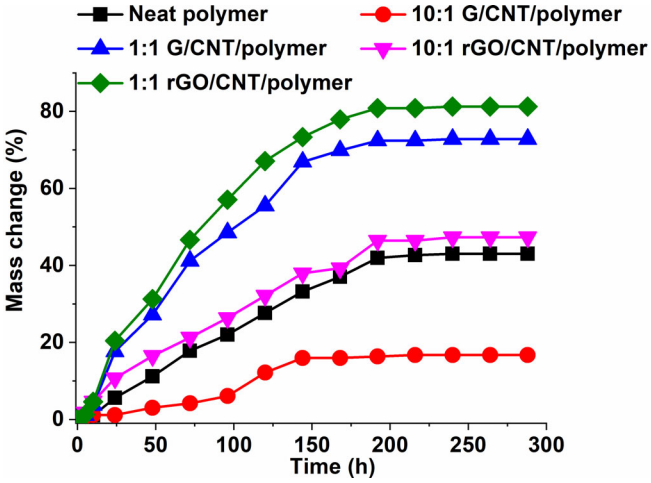

FIGURE 7 Mass change (%) in relation to the immersion time for the neat polymer and the different composite films.

carbon nanomaterials that are known for their excellent mechanical properties. The efficient stress transfer is related to the distribution of the filler, as well its chemical characteristics. In relation to this, the good dispersion of the 10:1 G/CNT hybrid throughout the polymer matrix improves the stress distribution leading to this composite having better properties than the 1:1 G/CNT composite, where filler agglomeration was observed. In the case of the rGO/CNT/polymer composites, it can be seen that these samples materials have better mechanical properties compared to the G/CNT/polymer. This is due to the fact that in the structure of rGO there are defects as well as oxygen functional groups that increase the compatibility of the filler with the polymer. Improved compatibility results in the formation of stronger interactions between the two phases and subsequently improving the stress transfer.

Along to high mechanical resistance, the low sensitivity to humidity and water is important property that can determine the application of polymer composites. It was evaluated by immersing the composite film in water and following the weight change, which was result to water uptake by the film. Figure 7 shows the results of the water uptake measurement, that is, the weight change in relation to immersion time is given.

As shown in Figure 7, all present increased water uptake compared to the neat polymer, except 10:1 G/CNT based composite.

These results are rather surprising. In the waterborne films, due to the presence of surfactant and hydrophilic moieties from the initiator, the water uptake is usually high, as it can be seen for the neat polymer that presents 40% water absorption in 300 h. It was expecting that the fillers will introduce a kind of barrier to the diffusion of water, even in case of the hybrid based on rGO. Nevertheless, the present results show that water absorption by the composite films is higher, indicating presence of the hydrophilic paths or network that facilitates the water diffusion. This can be on one hand result on the high presence of hydrophilic oxygen groups in case of rGO, and on the other hand irregularities during film formation that result of formation of different micro cracks while water is evaporated.

TABLE 4 Reduction of water uptake for 10:1 G/CNT/polymer compared to the neat polymer.

Immersion time (h)	48	96	144	192	240
Reduction of water uptake (%)	72	72	52	61	61

To examine the water uptake reduction in case of 10:1 G/CNT/polymer composites with respect to neat polymer, the weight change (%) of the neat polymer and 10:1 G/CNT/polymer was compared in Table 4.

The results show that incorporation of 1 wt% 10:1 G/CNT hybrid filler within the polymer matrix influenced the water uptake more considerably the first 100 h of the aging process, as the water uptake reduction was a little bit more than 72%. Before the saturation stage for both samples, the reduction of water uptake was decreased to 51%–61%. At saturated conditions, the water uptake reduction was 61%.

Most likely, the good distribution of the 10:1 G/CNT hybrid throughout the polymer matrix (Figure 3A), contributes to the filler acting as a barrier that prevents water from penetrating the material, and simultaneously it contributes to formation of good quality film during the water evaporation.

The 10:1 G/CNT/polymer composite was previously reported to possess radical scavenging character, thus introduced in (meth)acrylic polymer film it reinforces the

photostability.[6] This characteristic, combined with improved mechanical resistance and reduced water absorption make this composite promising material for future application as a protective coating for outdoor use.

4 | CONCLUSIONS

In this work, an easy and fast method for synthesis of G/CNTs and rGO/CNT based waterborne polymer composites is shown. Main aim of the work was to compare the different types of graphene G and rGO and to study their effect on the properties and performance of the resulting waterborne polymer composite.

The hybrid filler was prepared by sonication of G and CNT and rGO and CNT in different weight ratios (10:1, 1:1, and 1:10). The TEM results confirmed that the G(rGO) platelets are well exfoliated and the CNTs are distributed onto their surface. By increasing the amount of CNTs (1:10 hybrids) the exfoliation worsens. Such fillers were used for the synthesis of the composites by miniemulsion polymerization, giving rise to hybrid aqueous dispersions. Polymer composite films were prepared from these dispersions by water evaporation at atmospheric conditions. G/CNT and rGO/CNT polymer composites with filler load of 1 wt% were synthetized via in-situ miniemulsion polymerization. Water was used as polymerization medium, making this technique not only ecofriendly, but also low cost for preparation of polymer composites with versatile possibility of application.

SEM images have shown that G/CNT hybrid fillers were distributed better in the polymer matrix, presenting more organized structure. The surface of the films presented smoother surface than in case of rGO/CNT based composites, due to the higher hydrophilicity of the last, which led to increased accumulation of rGO/CNT on the surface. As a consequence of such structures, G/CNT based composites presented improved mechanical properties and one order of magnitude higher Young's moduli, without important drop in the elongation at break. The water resistance as well was much better than that of rGO/CNT based composites, especially for 10:1 ratio of the G/CNT, which presented 60% lower water absorption than neat polymer.

The present results demonstrate that miniemulsion polymerization indeed is an excellent method of choice for in situ synthesis of waterborne polymer composites. Based on the mechanical performance, as well as the reduced water uptake these films have a great potential to be used as a protective coating.

DATA AVAILABILITY STATEMENT

The data that support the findings of this study are available from the corresponding author upon reasonable request.

ORCID

Jadranka Blazhevska Gilev https://orcid.org/0000-0002-0551-7784

REFERENCES

1. Kausar A. Poly(methyl methacrylate) nanocomposite reinforced with graphene, graphene oxide, and graphite: a review. *Polym-Plast Technol Mater*. 2019;58:821-842.
2. Arzac A, Leal GP, de la Cal JC, Tomovska R. Water-borne polymer/graphene nanocomposites. *Macromol Mater Eng*. 2017;302:1600315.
3. Mohan VB, Lau K-t, Hui D, Bhattacharyya D. Graphene-based materials and their composites: a review on production, applications and product limitations. *Compos B*. 2018;142:200-220.
4. Khan ZU, Kausar A, Ullah H. A review on composite papers of grapheneoxide, carbon nanotube, polymer/go and polymer/cnt: processing strategies, properties and relevance. *Polym-Plast Technol Eng*. 2016;55:559-581.
5. Prosheva M, Ehsani M, Perez BT, Blazevska Gilev J, Joseph Y, Tomovska R. Dry sonication process for preparation of hybrid structures based on graphene and carbon nanotubes usable for chemical sensors. *Nanotechnology*. 2021;32:215601.
6. Prosheva M, Aboudzadeh MA, Leal GP, BlazevskaGilev J, Tomovska R. High-performance UV protective waterborne polymer coatings based on hybrid graphene/carbon nanotube radicals scavenging filler. *Part Part Syst Charact*. 2019;36:1800555.
7. Li L, Xu L, Ding W, Lu H, Zhang C, Liu T. Molecular-engineered hybrid carbon nanofillers for thermoplastic polyurethane nanocomposites with high mechanical strength and toughness. *Compos B*. 2019;177:107381.
8. Chen J, Walther JH, Koumoutsakos P. Covalently bonded graphene–carbon nanotube hybrid for high-performance thermal interfaces. *Adv Funct Mater*. 2015;25:7539-7545.
9. Yousefi K. Graphene-carbon nanotube hybrids: synthesis and application. *J Environ Treat Tech*. 2021;9:224-232.
10. Xiang D, Zhang X, Han Z, et al. 3D printed high-performance flexible strain sensors based on carbon nanotube and graphene nanoplatelet filled polymer composites. *J Mater Sci*. 2020;55:15769-15786.
11. Zhang H, Zhang G, Tang M, et al. Synergistic effect of carbon nanotube and graphene nanoplates on the mechanical, electrical and electromagnetic interference shielding properties of polymer composites and polymer composite foams. *Chem Eng J*. 2018;353:381-393.
12. Faccini M, Bautista L, Soldi L, et al. Environmentally friendly anticorrosive polymeric coatings. *Appl Sci*. 2021;11:3446.
13. Argaiz M, Ruipérez F, Aguirre M, Tomovska R. Ionic interparticle complexation effect on the performance of waterborne coatings. *Polymers*. 2021;13:3098.
14. Cui G, Zhang C, Wang A, et al. Research progress on self-healing polymer/graphene anticorrosion coatings. *Prog Org Coat*. 2021;155:106231.
15. Ahmadi Y, Ahmad S. Recent progress in the synthesis and property enhancement of waterborne polyurethane nanocomposites: promising and versatile macromolecules for advanced applications. *Polym Rev*. 2019;60:226-266.
16. Zhu X, Ni Z, Dong L, et al. In-situ modulation of interactions between polyaniline and graphene oxide films to develop waterborne epoxy anticorrosion coatings. *Prog Org Coat*. 2019;133:106-116.

17. Zhu M, Li S, Sun Q, Shi B. Enhanced mechanical property, chemical resistance and abrasion durability of waterborne polyurethane based coating by incorporating highly dispersed polyacrylic acid modified graphene oxide. *Prog Org Coat*. 2022;170:106949.
18. Wang S, Hu Z, Shi J, et al. Green synthesis of graphene with the assistance of modified lignin and its application in anticorrosive waterborne epoxy coatings. *Appl Surf Sci*. 2019;484:759-770.
19. Zhou X, Huang H, Zhu R, Sheng X, Xie D, Mei Y. Facile modification of graphene oxide with lysine for improving anticorrosion performances of water-borne epoxy coatings. *Prog Org Coat*. 2019;136:105200.
20. Wang H, He Y, Fei G, et al. Functionalizing graphene with titanate coupling agents as reinforcement for one-component waterborne poly(urethane-acrylate) anticorrosion coatings. *Chem Eng J*. 2019;359:331-343.
21. Zhang F, Liu W, Liang L, et al. The effect of functional graphene oxide nanoparticles on corrosion resistance of waterborne polyurethane. *Colloids Surf A Physicochem Eng Asp*. 2020;591:124565.
22. Dichiara A, Yuan J-K, Yao S-H, Sylvestre A, Bai J. Chemical vapor deposition synthesis of carbon nanotube-graphene nanosheet hybrids and their application in polymer composites. *J Nanosci Nanotechnol*. 2012;12:693-640.
23. Kim J-Y, Kim TY, Suk JW, et al. Enhanced dielectric performance in polymer composite films with carbon nanotube-reduced graphene oxide hybrid filler. *Small*. 2014;10:3405-3411.
24. Kim J, Kim SW, Yun H, Kim BJ. Impact of size control of graphene oxide nanosheets for enhancing electrical and mechanical properties of carbon nanotube–polymer composites. *RSC Adv*. 2017;7:30221-30228.
25. Li W, Dichiara A, Bai J. Carbon nanotube–graphene nanoplatelet hybrids as high-performance multifunctional reinforcements in epoxy composites. *Compos Sci Technol*. 2013;74:221-227.
26. Shen X-J, Pei X-Q, Liu Y, Fu S-Y. Tribological performance of carbon nanotube–graphene oxide hybrid/epoxy composites. *Compos B*. 2014;57:120-125.
27. Hu H, Zhao L, Liu J, et al. Enhanced dispersion of carbon nanotube in silicone rubber assisted by graphene. *Polymer*. 2017;53:3378-3385.
28. Shi Q, Zhu A. Interface regulation of graphene/carbon nanotube on the thermal conductivity and anticorrosion performance of their nanocomposite. *Prog Org Coat*. 2020;140:105480.
29. Ivanova R, Kotsilkova R, Ivanov E, et al. Composition dependence in surface properties of poly(lactic acid)/graphene/carbon nanotube composites. *Mater Chem Phys*. 2020;249:122702.
30. Uyor UO, Popoola API, Popoola OM, Aigbodion VS. Influence of graphene–carbon nanotubes and processing parameters on electrical and dielectric properties of polypropylene nanocomposites. *J Compos Mater*. 2021;55:3013-3022.
31. Jia L-C, Yan D-X, Jiang X, et al. Synergistic effect of graphite and carbon nanotubes on improved electromagnetic interference shielding performance in segregated composites. *Ind Eng Chem Res*. 2018;57:11929-11938.
32. Yang Z, Liu H, Wu S, Tang Z, Guo B, Zhang L. A green method for preparing conductive elastomer composites with interconnected graphene network via Pickering emulsion templating. *Chem Eng J*. 2018;342:112-119.
33. Dunlop MJ, Bissessur R. Nanocomposites based on graphene analogous materials and conducting polymers: a review. *J Mater Sci*. 2020;55:6721-6753.
34. Arzac A, Leal GP, Fajgar R, Tomovska R. Comparison of the emulsion mixing and in situ polymerization techniques for synthesis of water-borne reduced graphene oxide/polymer composites: advantages and drawbacks. *Part Part Syst Charact*. 2014;31:143-151.
35. Patole AS, Patole SP, JungS-Y YJ-B, An J-H, Kim T-H. Self assembled graphene/carbon nanotube/polystyrene hybrid nanocomposite by in situ microemulsion polymerization. *Eur Polym J*. 2012;48:252-259.
36. Spasevska D, Blaževska-Gilev J, Fajgar R, Tomovska R. Water borne polymer/graphene composites: analysis of the thermal degradation process. *Technol Acta*. 2014;7:41-48.
37. Spasevska D, Leal GP, Fernández M, BlazevskaGilev J, Paulis M, Tomovska R. Crosslinked reduced graphene oxide/polymer composites via in situ synthesis by semicontinuous emulsion polymerization. *RSC Adv*. 2015;5:16414-16421.
38. Pérez-Martínez BT, Farías-Cepeda L, Ovando-Medina VM, Asua JM, Rosales-Marines L, Tomovska R. Miniemulsion copolymerization of (meth)acrylatesin the presence of functionalized multiwalled carbon nanotubes for reinforced coating applications. *Beilstein J Nanotechnol*. 2017;8:1328-1337.
39. Trajcheva A, Politakos N, Perez BT, Joseph Y, Blazevska Gilev J, Tomovska R. QCM nanocomposite gas sensors—expanding the application of waterborne polymer composites based on graphene nanoribbon. *Polymer*. 2021;213:123335.
40. Spasevska D, Daniloska V, Leal GP, Blazevska Gilev J, Tomovska R. Reactive emulsion mixing as a novel pathwaytoward water-borne reduced graphene oxide/polymer composites. *RSC Adv*. 2014;4:24477-24483.
41. Sadegh F, Politakos N, de San G, et al. A green synthesis of nanocatalysts based on reduced graphene oxide/magnetic nanoparticles for the degradation of acid red 1. *RSC Adv*. 2020;10:38805-38817.
42. Kostadinova T, Politakos N, Trajcheva A, Blazevska-Gilev J, Tomovska R. Effect of graphene characteristics on morphology and performance of composite noble metal-reduced graphene oxide Sers substrate. *Molecules*. 2021;26:4775.
43. Dos Santos FC, Harb SV, Menu M-J, et al. On the structure of high performance anticorrosive PMMA-siloxane-silica hybrid coatings. *RSC Adv*. 2015;5:106754-106763.
44. Feizi S, Mehdizadeh A, Hosseini MA, Jafari SA, Ashtari P. Reduced graphene oxide/polymethyl methacrylate (rGO/PMMA) nanocomposite for real time gamma radiation detection. *Nucl Inst Methods Phys Res A*. 2019;940:72-77.

SUPPORTING INFORMATION

Additional supporting information can be found online in the Supporting Information section at the end of this article.

How to cite this article: Prosheva M, Ehsani M, Joseph Y, Tomovska R, Blazhevska Gilev J. Waterborne polymer composites containing hybrid graphene/carbon nanotube filler: Effect of graphene type on properties and performance. *Polym Compos*. 2023;1-13. doi:10.1002/pc.27483